J Fluoresc (2015) 25:763–775
DOI 10.1007/s10895-015-1565-6

ORIGINAL PAPER

Synthesis, Photophysical and Redox Properties of the D–π–A Type Pyrimidine Dyes Bearing the 9-Phenyl-9*H*-Carbazole Moiety

Egor V. Verbitskiy[1,2] · Aleksandr V. Schepochkin[1] · Nadezhda I. Makarova[3] · Igor V. Dorogan[3] · Anatoly V. Metelitsa[3] · Vladimir I. Minkin[3,4] · Sergey A. Kozyukhin[5] · Victor V. Emets[6] · Vitaly A. Grindberg[6] · Oleg N. Chupakhin[1,2] · Gennady L. Rusinov[1,2] · Valery N. Charushin[1,2]

Received: 10 January 2015 / Accepted: 23 March 2015 / Published online: 31 March 2015

Abstract Novel donor-π-acceptor dyes bearing the pyrimidine unit as an electron-withdrawing group have been synthesized by using combination of two processes, based on the microwave-assisted Suzuki cross-coupling reaction and nucleophilic aromatic substitution of hydrogen. Spectral properties of the obtained dyes in six aprotic solvents of various polarities have been studied by ultraviolet–visible and fluorescence spectroscopy. In contrast to the absorption spectra, fluorescence emission spectra displayed a strong dependence from their solvent polarities. The nature of the observed long wavelength maxima has been elucidated by means of quantum chemical calculations. The electrochemical properties of these dyes have been investigated by using cyclic voltammetry, while their photovoltaic performance was evaluated by a device fabrication study. The experimental and calculation data show that all of the dyes can be regarded as potentially good photosensitizers for dye-sensitized solar cells.

Keywords Pyrimidine · Carbazole · Nucleophilic aromatic substitution of hydrogen · Solvatochromism · Dye-sensitized solar cells

Electronic supplementary material The online version of this article (doi:10.1007/s10895-015-1565-6) contains supplementary material, which is available to authorized users.

✉ Egor V. Verbitskiy
Verbitsky@ios.uran.ru

[1] I. Postovsky Institute of Organic Synthesis, Ural Branch of the Russian Academy of Sciences, S. Kovalevskoy Str., 22, Ekaterinburg 620137, Russia

[2] Ural Federal University, Mira St. 19, Ekaterinburg 620002, Russia

[3] Institute of Physical and Organic Chemistry, Southern Federal University, Stachki Av., 194/2, 344090 Rostov on Don, Russia

[4] Southern Scientific Center of the Russian Academy of Sciences, Chekhov St., 41, 344006 Rostov on Don, Russia

[5] Kurnakov Institute of General and Inorganic Chemistry, RAS, Moscow 119991, Russia

[6] Frumkin Institute of Physical Chemistry and Electrochemistry, RAS, Moscow 119071, Russia

Introduction

Solvatochromism can be defined as the phenomenon, whereby a compound, being dissolved in various solvents, exhibits different colors due to a change in absorption or emission spectra of the molecule [1]. Solvatochromic D–π–A charge transfer dyes have received a considerable attention due to a growing fundamental interest in photochemistry and their application as environmental probes [1, 2]. These dyes attract have been paid much attention because of their use for determination of solvent polarity [3], as well as their potential application as colorimetric chemosensors for volatile organic compounds [4, 5]. Charge transfer dyes have also been developed for use as photo- (PL) and electroluminescent (EL) materials in dye lasers [6, 7], sensors [8], switchable viscosity probes [9], dual-ion-switched molecular brakes [10], dye-sensitized solar cells (DSSCs) [11–13] and optical light emitting diodes (OLEDs) [14].

Pyrimidine is a highly π-deficient heterocyclic system, and its fragment can be used as an electron-withdrawing part in push-pull structures. The ability of both nitrogen atoms of the pyrimidine ring for protonation, hydrogen bond formation and chelation are also of great importance, since pyrimidine derivatives can be used for the formation of supramolecular

assemblies. In addition, π-conjugated compounds bearing the pyrimidine fragment have been studied as promising candidates to obtain functional photoelectric materials, due to the intriguing structural and electronic properties of the pyrimidine ring [15–22]. During the last decade, hundreds of pyrimidine chromophores have been designed. In particular, numerous aryl substituted pyrimidines have been studied as fluorescent dyes [23–25]. Moreover, it should be noted that arylvinyl pyrimidines are now considered as well established structures of two-photon absorption dyes [26–28]. Some pyrimidine derivatives exhibit also the second order nonlinear optical properties [28–31].

It has been shown that combinations of the pyrimidine fragment with triphenylamine or carbazole units can give materials with excellent fluorescence properties. Indeed, elementary pyrimidine-triphenylamine **(I)** and pyrimidine-carbazole **(II)** dyads have been obtained and used as luminescent materials, exhibiting good solvability, film forming, high stability, and quantum efficiency (Fig. 1) [32, 33]. In addition, diphenyl-(4-pyrimidin-4-yl)-amine (I) was examined as a fluorescent ratiometric chemosensor for Hg^{2+} [34]. Recently, we have obtained six donor-π-acceptor organic dyes (IIIa-c and IVa-c), bearing the pyrimidine anchoring group as potentially good photosensitizers for dye-sensitized solar cells [13].

In continuation of this work we have elucidated solvatochromic properties of three pigments (**3a–c**) with 9-phenyl-9*H*-carbazole (donor) and pyrimidine (acceptor) fragments linked to each other through thiophenyl, 2-phenylthiophenyl and 2,2′-bithiophenyl groups (Scheme 1). The static and time-dependent density functional theory (TDDFT) calculations in ground and excited states have been used to analyze the solvatochromism observed in various solvents. The data derived from optical and electrochemical studies, and quantum calculations show that all compounds are potentially good photosensitizers for dye-sensitized solar cells.

Experimental Section

General Information

All reagents and solvents were purchased from commercial sources and dried by using standard procedures before use. 1, 4-Dioxane and H_2O for the microwave-assisted cross-coupling reaction were deoxygenated by bubbling argon for 1 h. 9*H*-Carbazole-9-(4-phenyl) boronic acid pinacol ester **(1)** and titanium (IV) oxide, anatase (nanopowder, <25 nm particle size) were purchased from Sigma-Aldrich. 4-(5-Bromothiophen-2-yl) pyrimidine **(2a)**, 4-[5-(4-bromophenyl) thiophen-2-yl] pyrimidine **(2b)** and 4-(5′-bromo-[2,2′] bithiophenyl-5-yl) pyrimidine **(2d)** were prepared according to the earlier reported procedure [13].

Melting points were determined on Boetius combined heating stages and were not corrected. Elemental analysis was carried on a Eurovector EA 3000 automated analyzer. ^1H and ^{13}C NMR spectra were recorded on an AVANCE-500 instruments using Me_4Si as an internal standard. The GC-MS analysis of all samples was carried out using an Agilent GC 7890A MS 5975C Inert XL EI/CI GC-MS spectrometer with a quadrupole mass-spectrometric detector with electron ionization (70 eV), and scan over the total ionic current in the range m/z 20÷1000 and a quartz capillary column HP-5MS (30 m×0.25 mm, film thickness 0.25 mm). Helium served as a carrier gas, the split ratio of the flow was 1: 50, and the consumption through the column was 1.0 mL min^{-1}; the initial temperature of the column was 40 °C (storage 3 min), programming rate was 10 °C min^{-1} to 290 °C (storage

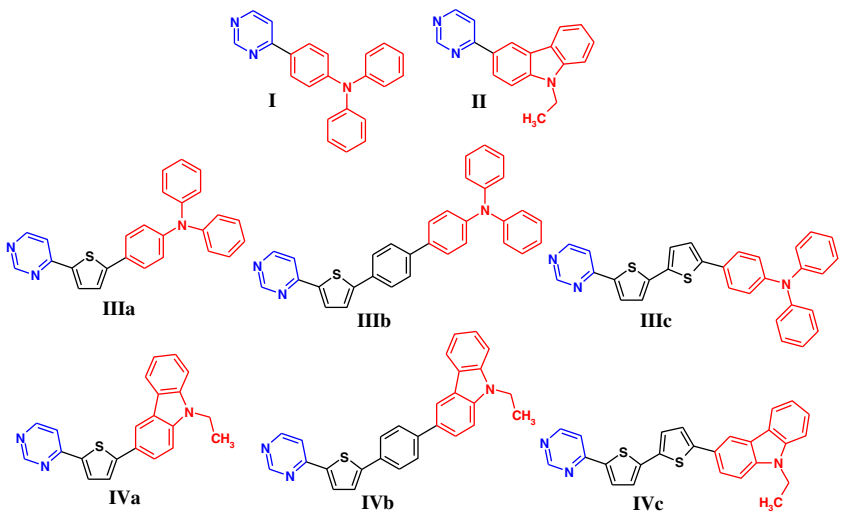

Fig. 1 Molecular structures of triphenylamine and carbazole dyes containing the pyrimidine ring as an electron-withdrawing group

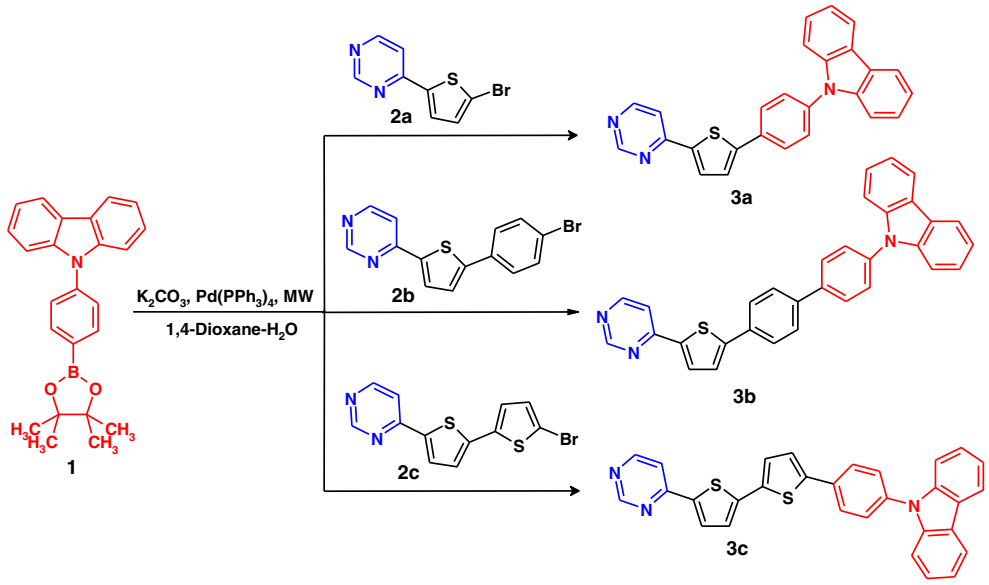

Scheme 1 Synthesis of the 9-phenyl-9*H*-carbazole-π-linker-pyrimidine dyes **3a–c**

20 min), the temperature of the evaporator was 250 °C, the temperature of the source was 230 °C, the temperature of the quadrupole was 150 °C, and the temperature of the transition chamber was 280 °C. Solutions of the samples with a concentration of 3–4 mg mL^{-1} were prepared in THF. Samples of the obtained solutions (1 mL) were analyzed.

Column chromatography was carried out using Alfa Aesar silica gel 0.040–0.063 mm (230–400 mesh), eluting with ethyl acetate-hexane. The progress of reactions and the purity of compounds were checked by TLC on Sorbfil plates (Russia), in which the spots were visualized with UV light (λ 254 or 365 nm).

Microwave experiments were carried out in a Discover unimodal microwave system (CEM, USA) with a working frequency of 2.45 GHz and the power of microwave radiation ranged from 0 to 300 W. The reactions were carried out in a 10 mL reaction tube with the hermetic Teflon cork. The reaction temperature was monitored using an inserted IR sensor for the external surface of the reaction vessel.

Redox and Spectroscopic Properties

Cyclic voltammetry was carried out on a Metrohm Autolab PGSTAT128N potentiostat with a standard three-electrode configuration. Typically, a three electrodes cell equipped with a glass carbon working electrode, $Ag/AgNO_3$ (0.01 M in anhydrous acetonitrile) reference electrode, and a glass carbon rod counter electrode was employed. The measurements have been carried out in anhydrous dichloromethane with tetrabutylammonium tetrafluoroborate (0.1 M), as the supporting electrolyte under an argon atmosphere at a scan rate of 100 mV/s. The potential of $Ag/AgNO_3$ reference electrode was calibrated by using the ferrocene/ferrocenium redox couple (Fc/Fc^+), which has the known oxidation potential of + 4.8 eV. The HOMO energy values were estimated from the onset potentials (E_{ox}^{onset}) of the first oxidation event according to the following equation:

$$E_{HOMO}(eV) = -\left[E_{ox}^{onset} - E_{1/2}(Fc/Fc+) + 4.8\right]$$

where $E_{1/2}(Fc/Fc^+)$ is the half-wave potential of the Fc/Fc^+ couple against the Ag/Ag^+ electrode.

UV/vis spectra were recorded for a 2×10^{-5} M solution with Varian Cary 100 spectrophotometer. Photoluminescent spectra were recorded for a 1×10^{-6} M solution on a Varian Cary Eclipse fluorescence spectrophotometer. UV/vis and fluorescence spectra were recorded using standard 1 cm quartz cells at room temperature. Stokes shifts were calculated considering the lowest energetic absorption band.

Comparative study of the photostability of the obtained compounds and commercial colorant POPOP (1,4-bis (5-phenyloxazol-2-yl) benzene) («Alfa Aesar») has been performed. Toluene solutions of the novel dyes and POPOP were irradiated with UV light at wavelength 365 nm for 1 h. Initial optical density of all solutions at wavelength 365 nm was equal to the same value (0.102). Fluorescence spectra of the dyes were recorded with 10 min interval between exposures, and their intensity were fixed at the maximum of the band. Photolysis of the solutions was carried out using "Newport" system on the basis of a mercury lamp (200 W) with a set of interference filters. The intensity of the optical radiation determined by the optical power meter "Newport 2935" at 365 nm was equal to 3.2×10^{16} photon·s^{-1}.

IR spectra of the dye powders and dyes adsorbed on TiO_2 nanoparticles were recorded on a Spectrum One Fourier transform IR spectrometer (Perkin Elmer) equipped with a diffuse reflectance attachment (DRA)

in the frequency range 420–3600 cm^{-1}. Spectrum processing and band intensity determination were carried out using the special software supplied with the spectrometer.

Molecular Orbital Calculation

Quantum chemical calculations were performed using the Gaussian 09 program [35]. The ground and first singlet excited state structures of the pyrimidine dyes were optimized using CAM-B3LYP [36] long range corrected functional with the 6-311+G(d,p) basis set. CPCM solvation model [37] with parameters corresponded to toluene (ε=2.38), dichloromethane (ε=8.93) and DMSO (ε=47.24) was used to account for the solvent. The time depended density functional theory (TD DFT) with state-specific methodology [38] was applied for calculation of absorption and emission spectra.

Fabrication of DSSCs

We used the photoanodes which were prepared on the TCO22-15 glass (Solaronix). Application of Ti-Nanoxide D/SP paste (Solaronix), comprising a nanocrystalline titanium dioxide, was performed by the standard «doctor blade» procedure, the thickness of thus obtained titanium dioxide film was 10 μm. Sensitizing of titanium dioxide was performed by soaking photoanodes in ~$3 \cdot 10^{-4}$ M methanol solutions of dye for 24 h. A three electrode photoelectrochemical cell (PECC-2, Zahner Elektrik) cell was used for the photoelectrochemical measurements. The photoanode served as the working electrode and a platinum wire with the surface area of 5 cm^2 was used as the auxiliary electrode. The voltammetric measurements were performed with an IPC Pro MF potentiostat under AM 1.5 global one sun of illumination (100 mW cm^{-2}) provided by a solar simulator (Newport 96000). The illumination power at different distances was determined with a Nova apparatus (OPHIR-SPIRICON Inc.). The illuminated photoanode area was 1.0 cm^2. The illumination was performed from the side of TiO_2 photoanode with the adsorbed dye. The time dependence of the photoanode and cathode potentials under the open-circuit conditions and the photocurrents at the short-circuit potential (transients) were measured under the illumination and at dark.

General Procedure for the Microwave-Assisted Suzuki Cross-Coupling Reactions

A solution of K_2CO_3 (207 mg, 1.5 mmol) in H_2O (3 mL) was added to a mixture of a bromo substituted pyrimidine (2a, 2b or 2c) (0.5 mmol), 9*H*-carbazole-9-(4-phenyl) boronic acid pinacol ester (1) (222 mg, 0.6 mmol) and Pd $(PPh_3)_4$ (58 mg, 10 mol %) in 1,4-dioxane (4 mL). The resulting mixture was irradiated in a microwave apparatus at 160 °C (250 W) for 30 min. After that solvent was distilled off *in vacuo*, and the residue was purified by flash column chromatography (hexane/ethyl acetate, 1:2) to afford the desired cross-coupling products (3a–c).

9-[4-(5-Pyrimidin-4-yl-Thiophen-2-yl)-Phenyl] -9H-Carbazole **(3a)**

The Suzuki cross-coupling reaction of 4-(5-bromothiophen-2-yl) pyrimidine **(2a)** with 9*H*-carbazole-9-(4-phenyl) boronic acid pinacol ester **(1)** (which has been performed according to the general procedure) gave after purification by column chromatography 149 mg (89 %) of 3a as a yellow solid. Melting point: 213–215 °C. ^{1}H NMR (500 MHz, DMSO-d_6) δ (ppm): 7.32 (ddd, *J*=7.9, 6.4, 1.6 Hz, 2H), 7.44–7.50 (m, 4H), 7.72–7.77 (m, 2H), 7.82 (d, *J*=4.0 Hz, 1H, H-3′), 8.07–8.09 (m, 3H), 8.18 (d, *J*=4.0 Hz, 1H, H-4′), 8.27 (d, *J*=7.9 Hz, 2H), 8.83 (d, *J*=5.4 Hz, 1H, H-6), 9.14 (d, *J*=1.3 Hz, 1H, H-2); ^{13}C NMR (126 MHz, DMSO-d_6) δ (ppm): 109.72, 115.25, 120.25, 120.55, 122.86, 126.00, 126.33, 127.27, 127.32, 130.39, 132.12, 136.92, 139.88, 140.98, 146.93, 157.60 (C-6), 157.78 (C-4), 158.75 (C-2); Anal. Calcd for $C_{26}H_{17}N_3S$ (403.51): C, 77.39; H, 4.25; N, 10.41. Found: C, 77.19; H, 4.05; N, 10.47. FT-IR (DRA, cm^{-1}): 422, 478, 531, 569, 622, 629, 642, 662, 725, 752, 771, 806, 834, 854, 914, 954, 983, 996, 1016, 1088, 1121, 1172, 1189, 1228, 1287, 1305, 1319, 1336, 1365, 1386, 1451, 1463, 1479, 1491, 1517, 1537, 1569, 1598, 1777, 1911, 2346, 3024, 3052.

9-[4′-(5-Pyrimidin-4-yl-Thiophen-2-yl)-Biphenyl-4-yl] -9H-Carbazole **(3b)**

The Suzuki cross-coupling reaction of 4-[5-(4-bromophenyl) thiophen-2-yl] pyrimidine **(2b)** with 9*H*-carbazole-9-(4-phenyl) boronic acid pinacol ester **(1)** (see the general procedure) gave after purification by column chromatography 115 mg (61 %) of 3b as a yellow solid. Melting point: 307–308 °C. ^{1}H NMR (500 MHz, $CDCl_3$) δ (ppm): 7.29–7.33 (m, 2H), 7.42–7.51 (m, 5H), 7.60 (dd, *J*=5.4, 1.3 Hz, 1H, H-5), 7.66–7.69 (m, 2H), 7.75–7.88 (m, 7H), 8.17 (d, *J*=7.8 Hz, 2H), 8.70 (d, *J*=5.4 Hz, 1H, H-6), 9.17 (d, *J*=1.3 Hz, 1H, H-2); ^{13}C NMR (126 MHz, $CDCl_3$) δ (ppm): 109.28, 114.93, 120.08, 120.36, 123.53, 124.55, 126.01, 126.04, 126.56, 127.46, 127.73, 128.32, 128.77, 129.10, 133.02, 137.32, 139.27, 140.33, 140.86, 140.95, 148.75, 157.13, 158.69 (C-6), 159.14 (C-4), 159.17 (C-2); Anal. Calcd for $C_{32}H_{21}N_3S$ (479.61): C, 80.14; H, 4.41; N, 8.76. Found: C, 79.81; H, 4.27; N, 8.75. FT-IR (DRA, cm^{-1}): 626, 660, 677, 695, 727, 741, 752, 769, 810, 917, 936, 959, 983, 1000, 1020, 1118, 1148, 1183,1235, 1278, 1317, 1335, 1369, 1385, 1400, 1453, 1464, 1477, 1502, 1519, 1537, 1573, 1569, 1624, 1643, 1734, 1793, 1910, 2926, 3048.

Table 1 UV/vis and photoluminescence data of dyes 3a–c in various aprotic solvents

Dye	Solvent E_T (30)[a] (kcal·mol^{-1})	Absorption λ_{max} (nm)/ε (10^3 M^{-1}·cm^{-1})	Photoluminescence			Stokes shift $\Delta\nu_{St}$ (cm^{-1})
			Excitation λ_{max} (nm)	Emission λ_{max} (nm)	Φ_F[b]	
3a	*n*-Heptane[c] 31.1	362, 291, 236	363, 291, 236	406, 428	0.62	2994
3b		353, 292, 233	351, 292, 233	407, 428	0.55	3759
3c		389, 291, 234	390, 291, 234	447, 474	0.07	3336
3a	Toluene 33.9	366 (29.6), 292 (19.2)	365, 292	429	0.91	4012
3b		364 (46.6), 293 (24.5)	364, 392	422	0.57	3776
3c		400 (43.2), 293 (22.05)	398, 293	465	0.19	3495
3a	Chloroform 39.1	366 (33.65), 292 (21.95)	365, 292	467	0.75	5909
3b		366 (55.2), 293 (29.45)	366, 293	458	0.60	5488
3c		402 (45.85), 293 (22.3)	400, 292	492	0.36	4550
3a	Dichloromethane 40.7	363 (36.5), 292 (22.65)	364, 292	472	0.74	6362
3b		363 (57.6), 292 (29.25)	364, 292	462	0.65	5903
3c		399 (45.45), 292 (22.2)	398, 292	494	0.35	4820
3a	Acetone 42.2	359 (36.7)	360	477	0.71	6891
3b		361 (39.25)	362	470	0.59	6424
3c		395 (45650)	395	492	0.29	4991
3a	DMSO 45.1	367 (38.75), 292 (23.65)	365, 292	498	0.65	7168
3b		368 (46.45), 293 (23.85)	367, 293	500	0.52	7174
3c		405 (46.3), 293 (23.6)	405, 293	512	0.51	5160

[a] Dimroth-Reichardt polarity parameter, kcal mol^{-1} [1]

[b] Fluorescence quantum yield determined relative to quinine bisulfate in 0.1 N H_2SO_4 as standard (Φ_F=0.52); excitation at 365 nm [39]

[c] Poorly soluble

9-[4-(5'-Pyrimidin-4-yl-[2,2'] Bitiophenyl-5-yl)-Phenyl] -9H-Carbazole **(3c)**

The Suzuki cross-coupling reaction of 4-(5′-bromo-[2,2′] bithiophenyl-5-yl) pyrimidine **(2c)** with 9*H*-carbazole-9-(4-phenyl) boronic acid pinacol ester (1) (see the general procedure) gave after purification by column chromatography 76 mg (67 %) of 3c as a yellow solid. Melting point: 245–247 °C. ^{1}H NMR (500 MHz, $CDCl_3$) δ (ppm): 7.28–7.33 (m, 3H), 7.36 (dd, *J*=13.0, 3.8 Hz, 2H), 7.42–7.48 (m, 4H), 7.57 (dd, *J*=5.4, 1.2 Hz, 1H, H-5), 7.61–7.64 (m, 2H), 7.72 (d, *J*= 4.0 Hz, 1H), 7.83–7.86 (m, 2H), 8.16 (d, *J*=7.8 Hz, 2H), 8.69 (d, *J*=5.4 Hz, 1H, H-6), 9.15 (d, *J*=1.2 Hz, 1H, H-2); ^{13}C NMR (126 MHz, $CDCl_3$) δ (ppm): 109.76, 114.85, 120.14, 120.36, 123.50, 124.55, 124.75, 126.00, 126.03, 127.04, 127.49, 128.51, 132.78, 136.43, 137.28, 140.24, 140.66, 142.11, 143.52, 157.07 (C-6), 158.42 (C-4), 159.11 (C-2); Anal. Calcd for $C_{30}H_{19}N_3S_2$ (485.63): C, 74.20; H, 3.94; N, 8.65. Found: C, 74.22; H, 3.83; N, 8.54. FT-IR (DRA, cm^{-1}): 623, 641, 657, 667, 725, 747, 765, 796, 834, 878, 914, 960, 993, 1017, 1085, 1110, 1120, 1148, 1171, 1230, 1284, 1306, 1316, 1335, 1365, 1386, 1414, 1451, 1470, 1509, 1530, 1573, 1595, 1624, 1759, 1908, 2927, 3059.

Results and Discussion

Materials Synthesis

The target compounds **3a–c** were prepared in good yields according to a procedure described in the previous publication [13]. The starting materials **2a**, **2b** and **2c** were coupled with 9*H*-carbazole-9-(4-phenyl) boronic acid pinacol ester **(1)** under microwave irradiation using 1,4-dioxane/H_2O (4:3) as solvent, K_2CO_3 and Pd (PPh_3) $_4$, as catalyst. All reactions studied proved to afford the corresponding 9-phenyl-9*H*-carbazole-π-linker-pyrimidine dyes 3a–c in 61–89 % yields within a reaction time not exceeding 30 min (Scheme 1).

The structural evidence for compounds **3a–c** has been obtained by elucidating their spectral data, including ^{1}H and ^{13}C NMR (see *Supporting Information*), and the data of elemental analysis.

Photophysical and Electrochemical Properties

The optical properties of the prepared donor-π-acceptor (D–π–A) type pyrimidine dyes containing 9-phenyl-9H-carbazole unit 3a–c have been elucidated by UV/vis and

photoluminescence (PL) spectroscopy in six aprotic solvents with different Dimroth-Reichardt polarity parameter ($E_T(30)$), notably *n*-heptane (31.1), toluene (33.9), chloroform (39.1), dichloromethane (40.7), acetone (42.2) and dimethyl sulfoxide (45.1) [1]. The results of these studies are summarized in Table 1.

The aim of this study was to explore the effect of solvent polarity on photophysical properties of these fluorophores, and to correlate these effects to their structures. The pyrimidine dyes **3a–c** have been established to show broad absorption maxima at the region of 353–405 nm (ε=19200–45650 $M^{-1}\cdot cm^{-1}$), which can be attributed to intramolecular charge-transfer excitation from the carbazole moiety to the pyrimidine ring (Table 1). The second and third absorption maxima proved to appear at 291–293 and 234–236 nm, respectively. UV–vis spectra for **3a–c** in various solvents are shown in Figs. S1, S2 and S3 (see Supplementary Material).

The D–π–A type pyrimidine dyes **3a–c** bearing the 9-phenyl-9*H*-carbazole unit exhibited blue-shifted absorption ($\Delta\lambda$= 21–36 nm in toluene) and fluorescence ($\Delta\lambda$=39–44 nm in toluene) emission spectra in comparison with the recently studied dyes of a similar structure on the basis of pyrimidine linked with the triphenylamine unit [13]. Since the ionization potential of carbazole is higher than that of triphenylamine, it can be suggested that a decrease in a donor ability of the D-fragment of dye is the reason of hypsochromic shift. Such dependence inherent for the absorption bands which are due to intramolecular charge transfer [40].

The structural modification of π-conjugated linker provides a significant influence on the absorption properties of the D–π–A derivatives **3a–c** (Table 1). An elongation of π-linker in the D–π–A molecules, such as 9-[4-(5′-pyrimidin-4-yl-[2,2′] bithiophenyl-5-yl)-phenyl]-9*H*-carbazole **3c**, by incorporating the second thiophene ring leads to a significant shift of the long-wavelength absorption ($\Delta\lambda_{max}$=27–38 nm) in comparison with 3a in all investigated solvents.

On the other hand, incorporation of the phenyl ring in the dye **3b** causes a hypsochromic shift of 9 nm in *n*-heptane and 2 nm in toluene, or a small bathochromic shift of 2 nm in other cases in comparison with those observed for compound 3a. Probably, it may be due to the disarranged π-conjugation in molecule 3b owing to nonplanar structure of the biphenyl fragment in solution [41].

It has been found that polarity of solvents exerts a weak influence on the long-wavelength absorption maxima of compounds 3a–c (Fig. 2). It can be attributed to a small change in dipole moments of the molecules in the excited Franck-Condon state.

Effective channel deactivation of electronic excitation energy of dyes **3a–c** is the fluorescence (Table 1, Figs. 3, S4 and S5). The excitation spectra proved to coincide with the absorption spectra (Table 1).

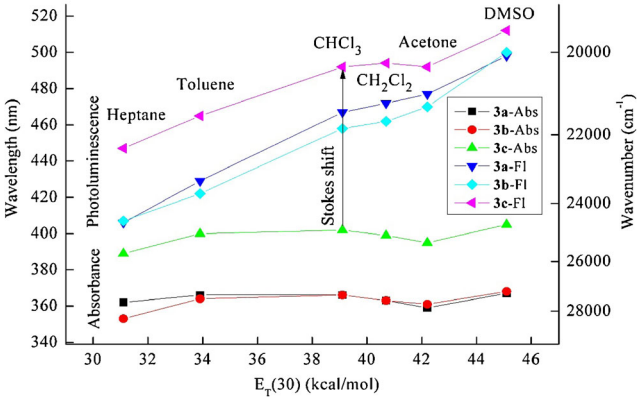

Fig. 2 Absorption end emission wavelength (λ_{max}) as a function of the Dimroth-Reichardt polarity parameter for dyes **3a–c**

Influence of the structure of dyes **3a–c** on the fluorescence spectra is similar to that on the absorption spectra. In contrast to the absorption spectra, fluorescence emission spectra exhibit a strong dependence from the solvent polarity (Table 1, Fig. 3).

The emission bands exhibit the red shifts with increasing of a solvent polarity and they cover a wide spectral range, providing solutions of various colors from blue to green (Fig. 4).

The observed correlation of the emission band wavelength with the solvent-dependent $E_T(30)$ Dimroth-Reichardt polarity parameter (see Fig. 1) is typical for compounds which undergo the intramolecular photoinduced electron transfer leading to a high polarity state which is stabilized by solvent [1, 42].

The Stokes shifts for **3a–c** are enhanced with increasing of solvent polarity from 2994 to 3759 cm^{-1} in *n*-heptane to 5160–7174 cm^{-1} in DMSO (Fig. 5).

High values of the Stokes shifts may be due to a remarkable change in dipole moments of dye molecules in the excited

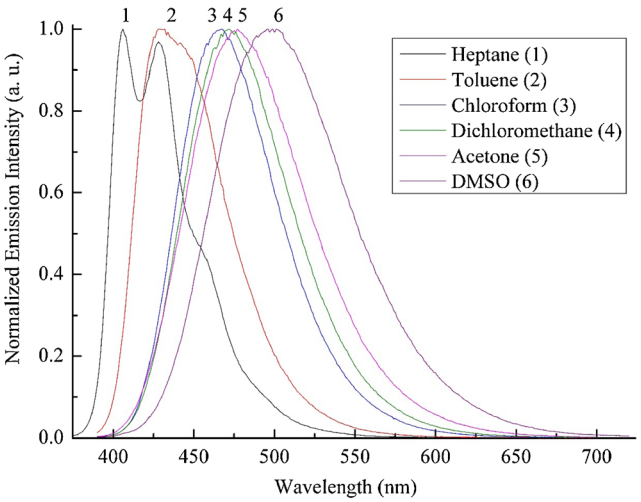

Fig. 3 Normalized emission spectra (λ_{ex}=365 nm) of compound **3a** in various solvents

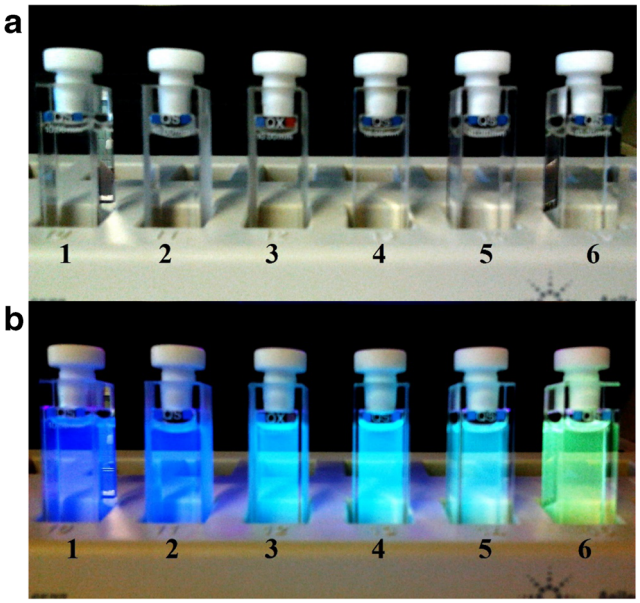

Fig. 4 Solutions photographs of dye **3a** in heptane (*1*), toluene (*2*), chloroform (*3*), dichloromethane (*4*), acetone (*5*) end DMSO (*6*): **a** before radiation (no emission); **b**) during radiation (emission, λ_{ex}= 365 nm) at room temperature

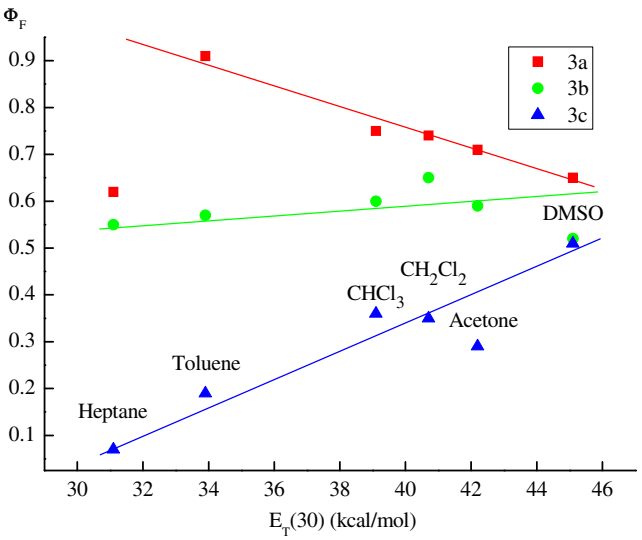

Fig. 6 Fluorescence quantum yield as a function of the Dimroth-Reichardt polarity parameter for dyes **3a–c**

state resulted from charge transfer from donor to acceptor fragment, which are accompanied by a compensatory relaxation of the solvent molecules [13, 42, 43].

An expansion of the π-linker by incorporating the additional thiophene ring leads to a significant bathochromic shift Δλ=12–43 nm) of the emission bands in comparison with compounds **3a** and **3b** (Table 1).

Quantum yields for fluorescence of dyes **3a–c** are strongly dependent on polarity of the solvents and their molecular structure, varying from 0.07 to 0.91 (Table 1). Thus, expansion of π-linker by incorporating the thiophene or phenyl rings results in a reduction of quantum yields of the photoluminescence.

With increase in polarity of the solvent quantum yields of the photoluminescence can be either reduced (see compound **3a**) or increased (compound **3c**) (Fig. 6).

To explain the observed behavior, non-radiative deactivation processes of the excited states should be taken into account. First of all, improving the efficiency of internal conversion results in a decrease in the energy gap S_0-S_1 of the irradiating structure for compounds 3a–c. On the other hand, an increase in structural flexibility of molecules with incorporation of the thienyl or phenyl fragments into π-linker leads to a smaller probability of non-irradiative processes for account of appearance of additional vibrational and rotational modes in the molecules. The difference in the character for the dependence of quantum yields for fluorescence of compounds **3a–c** from solvent polarity is a consequence of the impact of the above mentioned factors, operating in opposite directions with increasing a solvent polarity. Probably, decrease of the

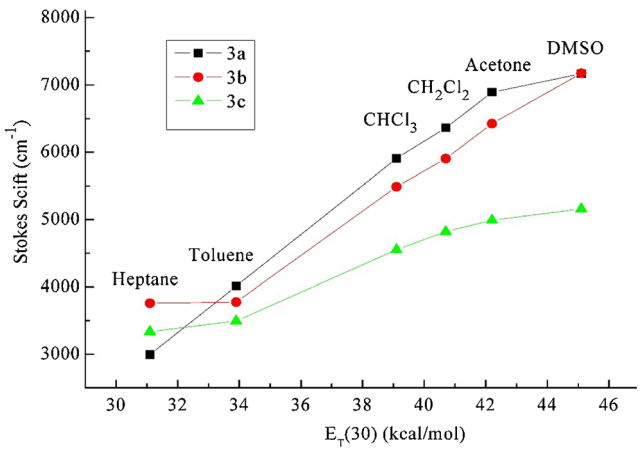

Fig. 5 The Stokes shifts as a function of the Dimroth-Reichardt polarity parameter for dyes **3a–c**

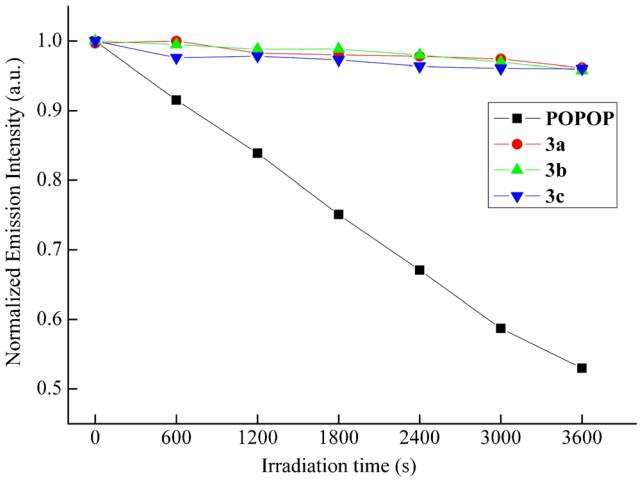

Fig. 7 Fluorescence intensity decay of compounds **3a–c** and POPOP when irradiated with light at 365 nm in toluene

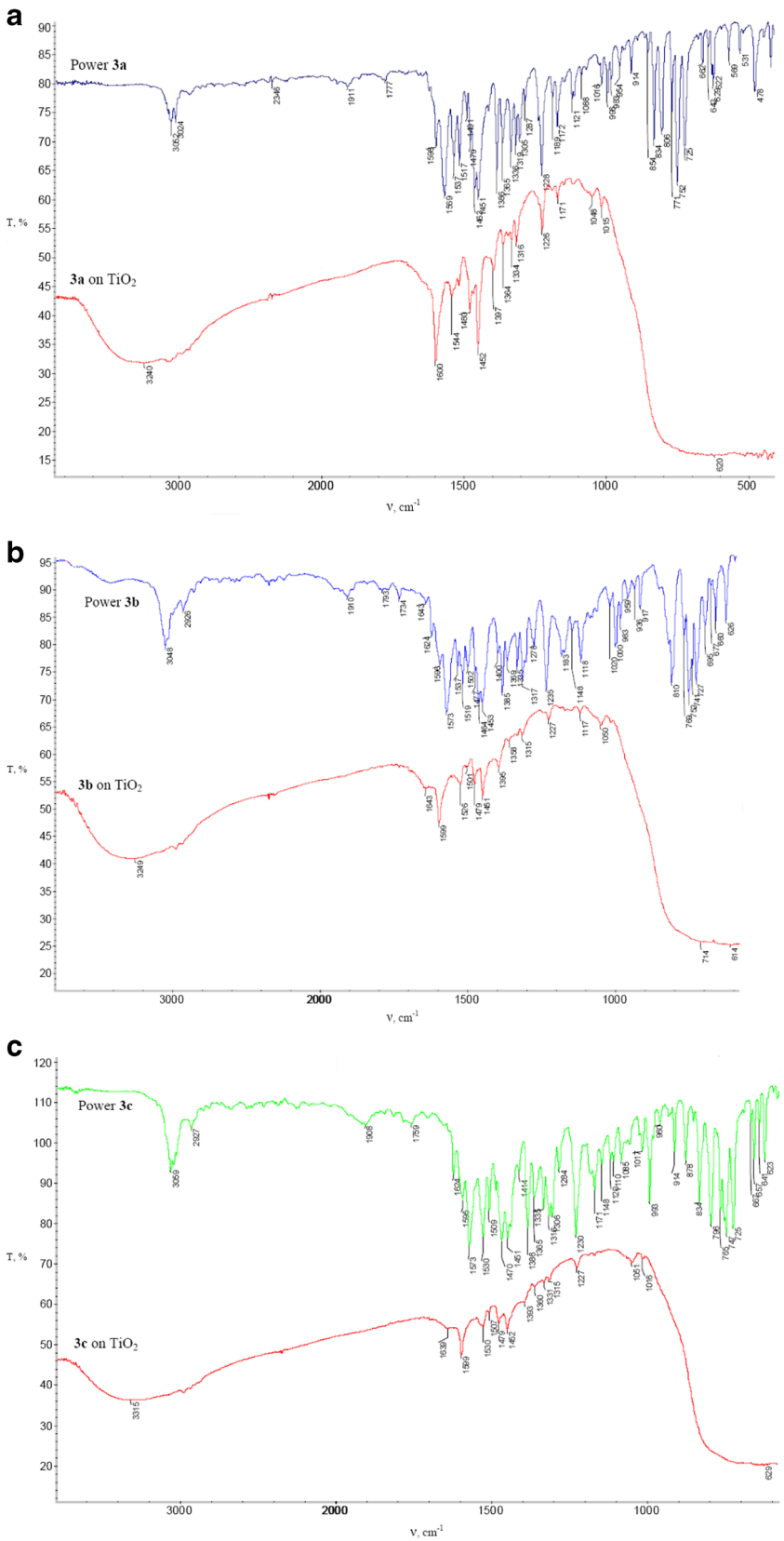

Fig. 8 FTIR spectra of dye powders and dyes adsorbed on TiO_2 nanoparticles for **a** 3a, **b** 3b and **c**) 3c

fluorescence efficiency with increasing of the solvent polarity in case of compound **3a** is due to a smaller energy gap S_0-S_1 of emitting state as a result of intramolecular charge transfer. In case of compounds **3b** and **3c** the major contribution to the

formation of radiative channel for deactivation of electronic excitation energy belongs to the processes which are connected with their greater structural flexibility in comparison with compound 3a. Namely, with increasing of the solvent polarity the stabilization of coplanar conformation in molecules 3b and 3c takes place. It enhances a probability for intramolecular charge transfer and forming of radiative state.

All compounds are photostable. Compounds **3a–c** show significantly higher resistance to photodegradation than luminophore POPOP. Irradiation of the solutions **3a–c** with light at 365 nm within 1 h leads to decreasing of the fluorescence intensity of not more than 5 %, while for POPOP similar figure is 47 % (Fig. 7).

Along with the certain spectroscopic properties an effective photosensitizers for dye-sensitized solar cells should possess a good adsorption to the TiO_2 nanoparticles. To prove the coordinating bonding of dyes **3a–c** on TiO_2 nanoparticles, we have measured the FTIR spectra of the dye powders and the dyes adsorbed on TiO_2 nanoparticles (Fig. 8). The characteristic C=N or C=C bands of the pyrimidine ring were clearly observed in the range of 1517–1537 and 1569–1573 cm^{-1}. When the dyes **3a–c** were adsorbed on the TiO_2 surface, the stretching hands observed at 1517–1537 and 1569–1573 cm^{-1} have disappeared and a new strong band appeared at 1599–1600 cm^{-1}, which can be assigned to pyrimidinyl groups coordinated to the Lewis acid sites on the TiO_2 surface. These consequences are in good agreement with a similar behavior of the pyridinyl anchoring group [44–50] and with our previous results for the pyrimidinyl anchoring group [13].

In order to investigate the electron transfer from the excited dye molecule to the conductive band of TiO_2, cyclic voltammetry (CV) was performed for these dyes in anhydrous CH_2Cl_2. The CV wave has been found to be not undergoing a substantial modification after repeated scans, thus revealing that all dyes were electrochemically stable under oxidative conditions. It is worth noting that the presence of a thiophene unit in the π-bridge of 3c decreases its oxidation potential (corresponding to the onset of the anodic event) of 0.96 V relative to dyes **3a** and **3b**. Since no cathodic behaviour of the dyes can be recorded by CV, their excited state oxidation potentials (corresponding to the LUMO energy levels) were calculated by adding the energy gap E_g (estimated from the onset of the absorption spectra recorded in CH_2Cl_2 solutions) to the HOMO energy values (Table 2). It should be noted that the obtained LUMO for all dyes (−2.33 to −2.63 eV) lay above the TiO_2 conduction band edge (~ −4.0 eV) warranting the necessary driving force for an efficient electron transfer process (Fig. 9). Although the HOMO level of dyes lays at −5.32 to −5.39 eV and slightly below experimentally obtained I_3^-/I^- redox potential (−4.8 eV), this width of the energy gap is sufficient for dyes regeneration process to take place. Thus, these compounds can potentially be used as sensitizing agents for DSSC.

Table 2 Electrochemical properties of 9-phenyl-9*H*-carbazole-π-pyrimidine **3a–c** derivatives

Dye	$E_{ox}^{onset\ a}$, V	E_{HOMO}, eV	$E_{LUMO}^{calc\ b}$, eV	E_g [c], eV
3a	1.03	−5.39	−2.36	3.03
3b	1.02	−5.38	−2.33	3.05
3c	0.96	−5.32	−2.63	2.69

[a] E_{ox}^{onset} – Onset oxidation potential

[b] $E_{LUMO}^{calc} = E_{HOMO} + E_g$

[c] E_g–Energy gap estimated from the onset of the absorption spectra recorded in CH_2Cl_2 solution

Computational Studies

To gain insight into the nature of the observed spectral properties of the dyes **3a–c** DFT calculations have been performed. The obtained results (Table 3, Fig. 10) show that long wavelength absorption maxima of **3a–c** at 366–405 nm are determined by S_0-S_1 transition with two nearly equal contributions. For compounds 3a and 3b the first one (HOMO – LUMO) can be assigned to intramolecular charge transfer (CT) from the carbazole fragment to the rest part of the molecule, while the second (HOMO-2 – LUMO) can be characterized as predominately π−π* transitions with a small amount of charge transfer. For **3c** the both contribution (HOMO – LUMO and HOMO-1 – LUMO) have a mixed (CT+π−π*) character associated with a redistribution of electron density within thiophene and phenyl fragments and accompanied by charge transfer from carbazole to the pyrimidine moiety.

It should be noted that preliminary results of the calculations with standard TDDFT hybrid functionals (PBE0, B3LYP) noticeably underestimate excitations energy of the first singlet excited state of **3a–c** due to fail to properly account for the 1/r dependence of CT excitations. To reduce this error, we employ a long-range corrected CAM-B3LYP functional for an improved assessment of CT states. On the other hand, inclusion of a long-range Hartree-Fock (HF) exchange into TDDFT manifested in the lowering of accuracy for

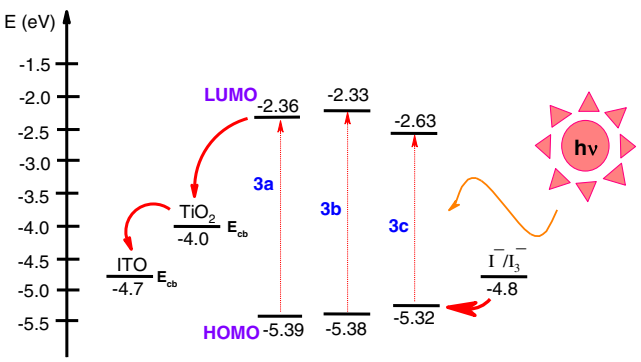

Fig. 9 Schematic energy diagram for dyes **3a–c**, a nanocrystalline TiO_2 electrode and I^-/I_3^- redox electrolyte

Table 3 Calculated excitation energies E^{calc} (eV) and oscillator strengths *f* of the S_0-S_1 transitions of 3a–c according to the TD PCM-CAM-B3LYP/6-311+G(d,p) calculation in toluene, dichloromethane and DMSO solutions. E^{exp} (eV) correspond to the observed long wavelength absorption maxima

Dye	Toluene			Dichloromethane			DMSO		
	E^{calc}, eV	*f*	E^{exp}, eV	E^{calc}, eV	*f*	E^{exp}, eV	E^{calc}, eV	*f*	E^{exp}, eV
3a	3.526	0.8631	3.397	3.625	0.9974	3.407	3.621	1.0134	3.397
3b	3.708	1.4129	3.407	3.645	1.4074	3.407	3.620	1.4051	3.379
3c	3.360	1.3974	3.116	3.330	1.3973	3.116	3.309	1.3968	3.062

locally excited states. So, systematic overestimation of the calculated excitation energies (Table 3) is most probably caused by the mixed nature of the S_0-S_1 transitions containing local excitation contributions. Nevertheless, the theoretical estimations of the transition energies are in a reasonable agreement with the experimental data.

According to the calculation results, electron density redistribution in **3a–c** upon excitation in the S_1 state leads to an increase of π-conjugation between thiophene and phenyl fragments of these molecules. As a result, molecular structures of **3a–c** in the first singlet excited state are significantly flattened compared to the ground state structures (Fig. S9 *in Supplementary Material*). These structural changes appear to cause the observed Stokes shifts.

Correct prediction of emission, as well as vertical excitation spectra, requires consideration of the excited state electronic density and the solvent reaction field in self-consistent manner. It is particularly important for a long range electron transfer processes, when variations of the dipole moments associated with electronic transitions are significant. For this reason, a more accurate and physically meaningful state-specific approach [38] has been used in a PCM TDDFT calculation, instead of standard linear response [51] method. Theoretically predicted emission energies (Table 4) are in a good agreement with the experimental data.

The visual representation of HOMO and LUMO orbitals (Fig. 10) of synthesized dyes clearly support the formation of push-pull system in molecules. A value for oscillator strengths (*f*) for the listed dyes (Table 3) implies that they have already a strongly delocalized π-system, but future modifications might be still desirable in order to increase the efficiency of newly synthesized dyes.

Photovoltaic Performance of the DSSC

Compound **3b** has been used as a photosensitizer for performance in trial DSSC because this dye has a maximum extinction coefficient in the solutions among studied dyes (see Table 1). Fig. 11 shows *I* – *V* characteristic of DSSC, fabricated on TiO_2 photoanodes with adsorbed **3b** dye upon illumination (100 mW×cm^{-2}). We used acetonitrile solution in the presence of 0.5 M LiI+0.05 M I_2 as a redox – system. The short circuit current density (I_{sc}) was 2.04 mA cm^{-2}, and the open circuit voltage (U_{oc}) was 0.525 V. The calculated power conversion efficiency of a cell (η) was 0.91 at a fill factor (*FF*) of 0.85.

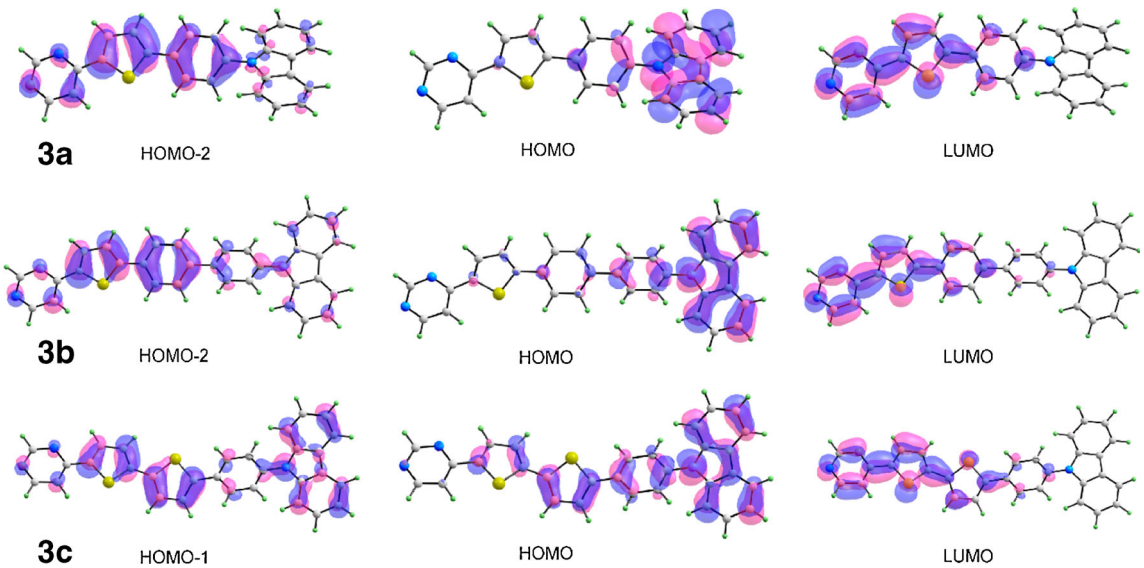

Fig. 10 The frontier molecular orbitals of **3a–c** involved in the S_0-S_1 transitions as calculated by the PCM-CAM-B3LYP/6-311+G (d,p) method (0.03 a.u. contour threshold has been used)

Table 4 Calculated emission energy E^{*calc} (eV) and oscillator strength *f* of the S_1-S_0 transitions of 3a–c according to the TD PCM-CAM-B3LYP/6-311+G(d,p) calculation in toluene, dichloromethane and DMSO solutions. E^{*exp} (eV) correspond to the observed emission maxima

Dye	Toluene			Dichloromethane			DMSO		
	E^{*calc}, eV	*f*	E^{*exp}, eV	E^{*calc}, eV	*f*	E^{*exp}, eV	E^{*calc}, eV	*f*	E^{*exp}, eV
3a	2.856	1.2112	2.890	2.600	1.2176	2.627	2.471	1.2155	2.490
3b	2.875	1.6133	2.938	2.734	1.6101	2.684	2.668	1.6106	2.480
3c	2.570	1.5273	2.546	2.460	1.5459	2.510	2.411	1.5553	2.422

In our opinion, low overall efficiency of DSSG is due the following reason. The absorption maximum of **3b** dye appears at the region 350–410 nm (see Fig. S2), and such position of the absorption band does not correspond to the maximum of the solar radiation spectrum.

Conclusion

Three novel 9-phenyl-9*H*-carbazole-π-pyrimidine dyes have been obtained through combination of the microwave-mediated Suzuki cross-coupling reaction and nucleophilic aromatic substitution of hydrogen (S_N^H).

All dyes exhibit a strong fluorescence with high quantum yields, and they demonstrate solvatochromic properties, thus allowing one to use these compounds as polarity sensors. Besides that, the scope of spectral, computational and electrochemical studies suggests that these dyes appear to be good photosensitizers in DSSC. Their LUMOs lay over the conduction band edge of TiO_2, while their HOMOs are under the reduction potential energy of the electrolytes (I^-/I_3^-), thus corresponding to the ability of electron transfer from the dye excited state to TiO_2 and charge regeneration after the photooxidation process, respectively. The photovoltaic measurements of these 9-phenyl-9*H*-carbazole-π-pyrimidine sensitizers in DSSC devices have shown to exhibit the conversion efficiency of 0.91 %, the fill factor (*FF*) of 85 %, the short-circuit photocurrent density (I_{sc}) of 2.04 mA cm^{-2}, the open-circuit voltage (U_{oc}) of 0.525 V for example of dye **3b**. Despite the fact that the described photovoltaic device showed relatively low efficiency coefficients, our studies open avenues for the development of organic dyes featuring azine as a new anchoring group. By appropriate structural modifications, electron-withdrawing pyrimidine can be developed, which may serve as an efficient anchoring group.

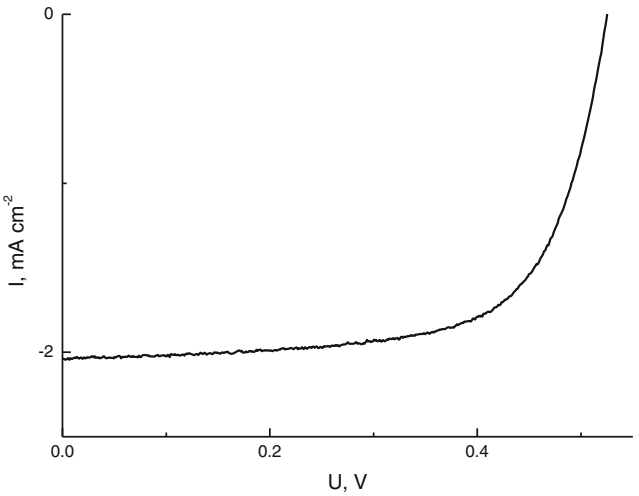

Fig. 11 Photocurrent density *vs* voltage for DSSC based on dye 3b under AM 1.5 G simulated solar light (100 mW cm^{-2})

Acknowledgments This work was supported by the Russian Foundation for Basic Research (research projects No. 13-03-96049-r_ural_a, 13-03-12434 ofi_м2, 13-03-90606-Arm_a, 14-03-01017-A, 14-03-00479-A and 14-03-31040-mol_a, 13-03-12415), the Council on Grants at the President of the Russian Federation (Program of State Support for Leading Scientific Schools of the Russian Federation and Young Scientists, Grant MK-3939.2014.3). N.I. Makarova, I.V. Dorogan, A.V. Metelitsa and V.I. Minkin would like to acknowledge the financial support of absorption, fluorescence and quantum chemical studies from the Ministry of Education and Science of Russian Federation in the framework of the State Assignment for Research project № 1895.

References

1. Reichardt C, Welton T (2011) Solvents and solvent effects in organic chemistry. WILEY-VCH Verlag GmbH & Co. KGaA, Weinheim
2. Marini A, Muñoz-Losa A, Biancardi A, Mennucci B (2010) What is solvatochromism? J Phys Chem B 114:17128–17135
3. Reichardt C (1994) Solvatochromic dyes as solvent polarity indicators. Chem Rev 94:2319–2358
4. Bamfield P (2001) Chromic phenomena: technological application of colour chemistry. The Royal Society of Chemistry, Cambridge
5. Janzen MC, Ponder JB, Bailey DP, Ingison CK, Suslick KS (2006) Colorimetric sensor arrays for volatile organic compounds. Anal Chem 78(11):3591–3600
6. Anthonov VS, Hohla KL (1983) Dye stability under excimer-laser pumping. Appl Phys B 32(1):9–14
7. Speiser S, Shakkour N (1985) Photoquenching parameters for commonly used laser dyes. Appl Phys B 38(3):191–197
8. de Silva AP, Gunaratne HQN, Gunnlaugsson T, Huxley AJM, McCoy CP, Rademacher JT, Rice TE (1997) Signaling recognition events with fluorescent sensors and switches. Chem Rev 97:1515–1566
9. Zhu LL, Li X, Ji FY, Ma X, Wang QC, Tian H (2009) Photolockable ratiometric viscosity sensitivity of cyclodextrine

polypseudorotaxane with light-active rotor graft. Langmuir 25: 3482–3486
10. Zhang D, Zhang Q, Su J, Tian H (2009) A dual-ion-switched molecular brake based on ferrocene. Chem Commun 1700–1702
11. Sansregret J, Drake JM, Thomas WRL, Lesiecki ML (1983) Light transport in planar luminescent solar concentrators: the role of DCM self-absorption. Appl Opt 22:573–577
12. Liu B, Zhu W, Zhang Q, Wu W, Xu M, Ning Z, Xie Y, Tian H (2009) Conveniently synthesized isophorone dyes for high efficiency dye-sensitized solar cell: tuning photovoltaic performance by structural modification of donor group in donor–π–acceptor system. Chem Commun :1766–1768
13. Verbitskiy EV, Cheprakova EM, Subbotina JO, Schepochkin AV, Slepukhin PA, Rusinov GL, Charushin VN, Chupakhin ON, Makarova NI, Metelitsa AV, Minkin VI (2014) Synthesis, spectral and electrochemical properties of pyrimidine-containing dyes as photosensitizers for dye-sensitized solar cells. Dyes Pigments 100: 201–214
14. Zhang XH, Chen BJ, Lin XQ, Wong QTY, Lee CS, Kwong HL, Lee ST, Wu SK (2001) A new family of red dopants based on chromen-containing compounds for organic luminescent device. Chem Mater 13(5):1565–1569
15. Gompper R, Mair H-J, Polborn K (1997) Synthesis of oligo(diazaphenyls). Tailormade fluorescent heteroaromatics and pathways to nanostructures. Synthesis 696–708
16. Kanbara T, Kushida T, Saito N, Kuwajima I, Kubota K, Yamamoto T (1992) Preparation and properties of highly electron-accepting poly(pyrimidine2,5-diyl). Chem Lett 583–586
17. Wong K-T, Hung T-S, Lin Y, Wu C-C, Lee G-H, Peng S-M, Chou CH, Su YO (2002) Suzuki coupling approach for the synthesis of phenylene-pyrimidine alternating oligomers for blue light-emitting material. Org Lett 4(4):513–516
18. Achelle S, Ramodenc Y, Marsais F, Plé N (2008) Star- and banana-shaped oligomers with a pyrimidine core: synthesis and light-emitting properties. Eur J Org Chem 3129–3140
19. Ortiz RP, Casado J, Hernández V, López Navarrete JT, Letizia JA, Ratner MA, Facchetti A, Marks TJ (2009) Thiophene-diazine molecular semiconductors: synthesis, structural, electrochemical, optical, and electronic structural properties; implementation in organic field-effect transistors. Chem Eur J 15(20):5023–5039
20. Kojima T, Nishida J, Tokito S, Yamashita Y (2009) New n-type field-effect transistors based on pyrimidine-containing compounds with (trifluoromethyl) phenyl groups. Chem Lett 38:428–429
21. Achelle S, Plé N (2012) Pyrimidine ring as building block for the synthesis of functionalized π-conjugated materials. Curr Org Synth 9:163–187
22. Achelle S, Baudequin C (2013) Recent advances in pyrimidine derivatives as luminescent, photovoltaic and non-linear optical materials. Targets Heterocycl Syst 17:1–34
23. Itami K, Yamazaki D, Yoshida J (2004) Pyrimidine-core extended π-systems: general synthesis and interesting fluorescent properties. J Am Chem Soc 126:15396–15397
24. Bagley MC, Lin Z, Pope SJA (2009) Barium manganate in microwave-assisted oxidation reactions: synthesis of solvatochromic 2,4,6-triarylpyrimidines. Tetrahedron Lett 50: 6818–6822
25. Tumkevičius S, Voitechovičius A, Adomėnas P (2012) Synthesis of novel 2,4,6-triarylpyrimidines. Chemija 23:61–67
26. Liu B, Hu XL, Liu J, Zhao YD, Huang ZL (2007) Synthesis and photophysical properties of novel pyrimidine-based two-photon absorption chromophores. Tetrahedron Lett 48:5958–5962
27. Li L, Ge J, Wu H, Xu QH, Yao SQ (2012) Organelle-specific detection of phosphatase activities with two-photon fluorogenic probes in cells and tissues. J Am Chem Soc 134:12157–12167
28. Achelle S, Malval JP, Aloïse S, Barsella A, Spangenberg A, Mager L, Akdas-Killig H, Fillaut JL, Caro B, Robin-le Guen F (2013) Synthesis, photophysics and nonlinear optical properties of stilbenoid pyrimidine-based dyes bearing methylenepyran donor groups. ChemPhysChem 14:2725–2736
29. Achelle S, Barsella A, Baudequin C, Caro B, Robin-le Guen F (2012) Synthesis and photophysical investigation of a series of push-pull arylvinyldiazine chromophores. J Org Chem 77:4087–4096
30. Castet F, Pic A, Champagne B (2014) Linear and nonlinear optical properties of arylvinyldiazine dyes: a theoretical investigation. Dyes Pigments 110:256–260
31. Denneval C, Achelle S, Baudequin C, Robin-le Guen F (2014) Prediction of photophysical properties of pyrimidine chromophores using Taguchi method. Dyes Pigments 110:49–55
32. Ling Q, Huang W, Mei Q, Weng J (2011) Preparation of 4-(hetero)-arylpyrimidins compounds as luminescent materials. Patent CN102206207
33. Weng J, Mei Q, Fan Q, Ling Q, Tong B, Huang W (2013) Bipolar luminescent materials containing pyrimidine terminals: synthesis, photophysical properties and a theoretical study. RSC Adv 3: 21877–21887
34. Weng J, Mei Q, Ling Q, Huang W (2012) A new colorimetric and fluorescence ratiometric sensor for Hg^{2+} based on 4-pyren-1-yl-pyrimidine. Tetrahedron 68:3129–3134
35. Frisch MJ, Trucks GW, Schlegel HB, Scuseria GE, Robb MA, Cheeseman JR, Scalmani G, Barone V, Mennucci B, Petersson GA, Nakatsuji H, Caricato M, Li X, Hratchian HP, Izmaylov AF, Bloino J, Zheng G, Sonnenberg JL, Hada M, Ehara M, Toyota K, Fukuda R, Hasegawa J, Ishida M, Nakajima T, Honda Y, Kitao O, Nakai H, Vreven T, Montgomery JA Jr, Peralta JE, Ogliaro F, Bearpark M, Heyd JJ, Brothers E, Kudin KN, Staroverov VN, Kobayashi R, Normand J, Raghavachari K, Rendell A, Burant JC, Iyengar SS, Tomasi J, Cossi M, Rega N, Millam NJ, Klene M, Knox JE, Cross JB, Bakken V, Adamo C, Jaramillo J, Gomperts R, Stratmann RE, Yazyev O, Austin AJ, Cammi R, Pomelli C, Ochterski JW, Martin RL, Morokuma K, Zakrzewski VG, Voth GA, Salvador P, Dannenberg JJ, Dapprich S, Daniels AD, Farkas O, Foresman JB, Ortiz JV, Cioslowski J, Fox DJ (2013) he molecular orbital calculation was carried out using the gaussian 09, revision D.01. Gaussian, Wallingford
36. Yanai T, Tew D, Handy N (2014) A new hybrid exchange-correlation functional using the Coulomb-attenuating method (CAM-B3LYP). Chem Phys Lett 393:51–57
37. Barone V, Cossi M (1998) Quantum calculation of molecular energies and energy gradients in solution by a conductor solvent model. J Phys Chem A 102(11):1995–2001
38. Improta R, Barone V, Scalmani G, Frisch MJ (2006) A state-specific polarizable continuum model time dependent density functional theory method for excited state calculations in solution. J Chem Phys 125:054103
39. Meech SR, Phillips D (1983) Photophysics of some common fluorescence standards. J Photochem 23:193–217
40. Barltrop JA, Coyle JD (1975) Excited states in organic chemistry. Wiley, London. New York, 376 p
41. Barich DH, Pugmire RJ, Grant DM (2001) Investigation of the structural conformation of biphenyl by solid state ^{13}C NMR and quantum chemical NMR shift calculations. J Phys Chem A 105: 6780–6784
42. Hadad C, Achelle S, Garcia-Martinez JC, Rodriguez-Lopez J (2011) 4-arylvinyl-2,6-di(pyridine-2-yl)pyrimidines: synthesis and optical properties. J Org Chem 76:3837–3845
43. Achelle S, Nouira I, Pfaffinger B, Ramondene Y, Ple N, Rodriguez-Lopez J (2009) V-shaped 4,6-Bis(arylvinyl)pyrimidine oligomers: synthesis and optical properties. J Org Chem 74:3711–3717
44. Ooyama Y, Nagano T, Inoue S, Imae I, Komaguchi K, Ohshita J, Harima Y (2011) Dye-sensitized solar cells based on donor-π-acceptor fluorescent dyes with a pyridine ring as an electron-

withdrawing-injecting anchoring group. Chem Eur J 17:14837–14843
45. Ooyama Y, Inoue S, Nagano T, Kushimoto K, Ohshita J, Imae I, Komaguchi K, Harima Y (2011) Dye-sensitized solar cells based on donor-acceptor π-conjugated fluorescent dyes with a pyridine ring as an electron-withdrawing anchoring group. Angew Chem Int Ed 50:7429–7433
46. Ooyama Y, Harima Y (2012) Photophysical and electrochemical properties, and molecular structures of organic dyes for dye-sensitized solar cells. Chem Phys Chem 13:4032–4080
47. Ooyama Y, Yamaguchi N, Imae I, Komaguchi K, Ohshita J, Harima Y (2013) Dye-sensitized solar cells based on D-π-A fluorescent dyes with two pyridyl groups as an electronwithdrawing-injecting anchoring group. Chem Commun 49:2548–2550
48. Harima Y, Fujita T, Kano Y, Imae I, Komaguchi K, Ooyama Y, Ohshita J (2013) Lewis-acid sites of TiO_2 surface for adsorption of organic dye having pyridyl group as anchoring unit. J Phys Chem C 117:16364–16370
49. Lu J, Xu X, Li Z, Cao K, Cui J, Zhang Y, Shen Y, Li Y, Zhu J, Dai S, Chen W, Cheng Y, Wang M (2013) Zinc porphyrins with a pyridine-ring-anchoring group for dye-sensitized solar cells. Chem Asian J 8:956–962
50. Ooyama Y, Hagiwara Y, Mizumo T, Harima Y, Ohshita J (2013) Photovoltaic performance of dye-sensitized solar cells based on D-π-A type BODIPY dye with two pyridyl groups. New J Chem 37:2479–2485
51. Cossi M, Barone V (2001) Time-dependent density functional theory for molecules in liquid solutions. J Chem Phys 115:4708–4717